


Chapter 3

The Call Admission Control for Uplink Dedicated and Shared Channels in Multimedia CDMA Cellular Systems



In this chapter, we propose intelligent call admission control for wideband CDMA cellular systems to support differentiated QoS requirements, guarantee the forced termination probability of handoffs, and maximize the spectrum utilization. The intelligent call admission controller (ICAC) contains a fuzzy call admission processor to make admission decision for a call request by considering QoS measures such as the forced termination (drop call) probability of handoff, the outage probability of all service types, the predicted next-step existing-call interference, the link gain, and the estimated equivalent interference of the call request. The pipeline recurrent neural network (PRNN) is used to accurately predict the next-step existing-call interference, and the fuzzy logic theory is applied to estimate the new/handoff call interference based on knowledge of effective bandwidth method. Simulation results indicate that ICAC achieves system capacity higher than conventional CAC schemes and can cope with the unpredictable statistical fluctuation in wireless environment; it always fulfill QoS requirements for all service types and keep the forced termination probability satisfied, while conventional CAC schemes does not.

3.1 Notation List of Chapter 3

We summarize the important notations of this chapter in the following table.

Table 3.1: Notation List of Chapter 3

Notation	Description
W	The bandwidth of the carrier of CDMA network
R_i	The basic transmission rate for traffic type i
SF_i	The spreading factor used by traffic type i
$I_k(n)$	The total received interference in the base station k at time n
$\bar{I}_k(n)$	The averaged total received interference in the base station k at time n
$\hat{\bar{I}}_k(n+1)$	The predicted averaged interference by PRNN predictor in the base station k at time n
$SIR_i(n)$	The received SIR connection i at frame time n
ρ_i	The ratio of the required γ_i^* of type i over the required γ_1^* of voice connections
P_i	The required received power at base station for connection i
S	The required received power level at base station for basic rate transmission
K	The number of cells in the considered system
$N_{i,k}$	The number of connections in traffic type i and cell k
R_p	The traffic parameter of peak rate for the new/handoff connection
R_m	The traffic parameter of mean rate for the new/handoff connection
T_p	The traffic parameter of peak rate duration for the new/handoff connection
I_{th}	The interference threshold in the uplink direction pre-planned at base station
$P_{otg,i}^*$	The QoS requirement of outage probability for traffic type i
$P_{p,i}^*$	The QoS requirement of packet dropping probability for type i
$P_{f,i}^*$	The QoS requirement of forced termination probability for traffic type k
γ_i^*	The SIR requirement of type i derived from the required E_b/N_0
$M_{i,k}$	The number of code channels used by connection i in the cell k
$\nu_{i,k}$	The type-1 voice activity variable used by connection i in the cell k
$\delta_{i,k}$	The type-2 data activity variable used by connection i in the cell k

Notation	Description
\hat{C}	The equivalent interference of the new/handoff connection output from FEIE
Z	The CAC decision output from ICAC controller
d	The distance from the new/handoff connection to the base station
d_0	The decay of correlation in correlated shadowing model
$L(d)$	The link gain model with distance d
$\zeta_{i,k}(d)$	The log-normal shadowing part of the link gain model
θ	The propagation decay factor
φ	The handoff margin in dB against the ping-pong effect
$T(X)$	The term set of input variable X used in Fuzzy logic
μ_X	The membership function of each term set for the input variable X
$h(\cdot)$	The trapezoidal function used as the membership function
$f(\cdot)$	The triangular function used as the membership function
p	The prediction order of PRNN interference predictor
$e_q(n)$	The error output of stage q of the PRNN interference predictor
$\vec{y}_q(n)$	The output vector of stage q of the PRNN interference predictor
$w_{i,j}$	The synaptic weighting from input node j to output node i of PRNN interference predictor



3.2 Introduction

With desired features such as high system capacity (soft capacity), low power transmission, soft hand-off, multipath mitigation, and interference suppression [6], [61], code division multiple access (CDMA) has been adopted for third generation wireless communication systems. The third generation wideband CDMA cellular system must be able to support integrated services applications [8] with differentiated *quality-of-service* (QoS) requirements. Furthermore, handoff is an important issue in WCDMA systems. Although soft handoff is the very desired feature of CDMA technology, the hard handoff is also the mandatory scheme in WCDMA systems. The forced termination probability should also be guaranteed to satisfy the user's requirement. Thus, a sophisticated call admission control (CAC) is needed so that the system can satisfy various QoS constraints such as the forced termination (drop call) probability for handoffs and the outage probabilities

for different services, and maximize the spectrum utilization.

Despite the extensive attention paid to the design of call admission control in CDMA systems, few investigations have considered the QoS requirement, resulting in a situation in which QoS requirements are not ensured. Liu and Zarki [9] proposed an uplink signal-to-interference (SIR)-based CAC, which adopted a *residual capacity* algorithm, for a DS-SS-SSMA cellular system with pure voice traffic. Yang and Geraniotis [10] derived optimal admission policies for integrated voice and data traffic in a CDMA packet radio network. Dziong, Jia, and Mermelstein [11] proposed an adaptive traffic admission control by estimating the uplink interference at the base station. It employed a linear Kalman filter driven by the interference measurement. These two CACs cannot keep QoS requirements guaranteed.

References [14]-[17] studied the QoS-based CAC. Kim, Shin, and Lee [14] extended the work in [9] but fulfilled the outage requirement. However, only single class of service was considered. With closed blocking probability performance, this scheme successfully kept the outage probability guaranteed. Ishikawa and Umeda [15] developed two strategies for CAC: one is based on the number of users and the other is based on the interference level. Although the theoretical expression for the blocking rate and the loss probability of communication quality as functions of traffic intensity and CAC threshold were obtained, integrated traffic and differentiated QoS requirements were not studied. Liu and Silvester [16] proposed a joint admission/congestion control for wireless CDMA systems supporting integrated services. An adaptive admission control policy was developed to adjust the priority of voice traffic, and a data traffic control scheme was adopted to maintain the packet error rate of real-time voice traffic, while allowing itself to utilize the residual channel capacity. However, the work focused mainly on designing an access control scheme based on the admitted number of users but not on the CAC policy. Evans and Everitt

[17] utilized an effective bandwidth concept [4] to transform the traffic generated by a user into an equivalently occupied bandwidth. The per class outage requirement was not supported, and the system state dimensions grew with an increasing number of cells, making the computational complexity intractable. Kim and Han [18] also proposed a CAC scheme which considered dual classes of services. This scheme measured the received interference and estimated the power requirement for the new user to predict the resulting SIR. The outage probability might overwhelm in some traffic load region. Other works, such as [26] and [27], focused on the resource allocation and provided simple admission conditions.

Also, there were literatures working on the CAC problem with further consideration of handoff protection. The handoff calls should be prioritized than new calls due to the requirement on forced termination probability. Shin, Cho, and Sung [28] proposed to reserve a number of radio channels to protect handoff calls in DS-CDMA cellular systems, where the amount of interference of a connection is quantized as one radio channel, and the system capacity is then regarded as a fixed number of radio channels. The number of reserved channels for handoff was derived according to the handoff rate and the arrival rate, as it was done in TDMA systems. The change of interference to the destination cell was not even considered. Kuo and Ko [29] adopted probability reservation concept for handoff calls to improve the call dropping probability. The probability reservation scheme reserves resource in all the possible cells for the call that will handover. This scheme was inefficient for radio resource management in CDMA environments. Jeon and Jeong [30] utilized the property of soft capacity in CDMA systems, and designed prioritization by setting SIR threshold of handoff calls lower than that of new calls. However, the forced termination probability still cannot be guaranteed. In the practical simulation model for CDMA system, i.e. the continuous movement of the mobile connection and the correlated

shadowing, we can find that the moving speed and the handoff margin will impact on the variation of mean interference and the capacity of a QoS guaranteed cellular system. Therefore, a more robust CAC scheme for hard handoff should be elaborately designed.

Interference in CDMA systems can be considered as an indication of system load, and handoff will not introduce more load to its destination cell. Due to one cell reuse property in CDMA systems, a mobile continues interfering every adjacent cell. As the user moves near a cell boundary, a margin of relative pilot strength is set to avoid ping-pong effect. If we observe the change of received interference by the destination cell before the handoff and after the handoff, the overall interference received by the destination cell will be lower after handoff in the most cases. From this point of view, CAC need not block the handoff call in the normal traffic condition. However, in the heavy load condition, handoff call may be blocked, and to guarantee the forced termination probability is still an important issue.

The wideband CDMA systems will turn out to be within a *dynamic, imprecise, and bursty environment* because of the *unpredictable statistical fluctuations* in the flow of wireless multimedia traffic. To the end, we here adopt intelligent techniques such as fuzzy logic systems and neural networks to cope with the traffic uncertainty. The fuzzy logic systems have replaced conventional technologies in many scientific applications and engineering systems, especially in control systems. They appear to provide a robust mathematical framework for dealing with real-world imprecision; and they can also provide decision support and expert systems with powerful reasoning capabilities bound by a set of fuzzy rules. When a mathematical model of a process does not exist, it is appropriate to use fuzzy logic systems. On the other hand, neural networks are information processing systems that are constructed to characterize the human brain. They are able to learn arbitrary nonlinear input-output mapping directly from training data; they can automatically ad-

just their connection weights to achieve optimality for controllers, predictors, etc. Both fuzzy logic and neural networks are numerical model-free and dynamical estimators. They can improve systems working in uncertain and unstationary environments.

Therefore, the chapter proposes an *intelligent call admission control* method for wide-band CDMA cellular systems to support differentiated QoS requirements such as the forced termination probability of handoffs and the outage probability for all service types, and maximize the spectrum utilization. The *intelligent call admission controller* (ICAC) has functional blocks of *fuzzy call admission processor* together with two pre-processors: *fuzzy equivalent interference estimator* and *PRNN interference predictor*. The *fuzzy equivalent interference estimator* employs the fuzzy logic theory to mimic domain knowledge contained in the effective bandwidth scheme proposed in [4], [5]. Doing so allows us to estimate the equivalent interference of a call request from its claimed traffic characteristics and QoS requirement. The *PRNN interference predictor* adopts a pipeline recurrent neural network [63] for accurately predicting the mean interference of existing calls. The *fuzzy call admission processor* adopts fuzzy logic control capable of providing decision support and expert system with powerful reasoning capability. The processor decides whether to accept the new or handoff call based on not only the estimated equivalent interference caused by the call and the predicted mean interference generated by existing calls but also the QoS measures such as the outage probabilities of all service types and the forced termination probability as system feedbacks. In addition, the link gain of the call request, denoting a good or bad user, is further considered.

The ICAC is justified by comparing it with some conventional CAC schemes such as the SIR-based CAC with intercell interference prediction (PSIR-CAC) proposed in [14] and the CAC of multimedia calls (MCAC) proposed in [30]. Simulation results indicate that ICAC can always fulfill the multiple QoS requirements under all traffic load conditions,

while these conventional CAC schemes fail in heavy traffic load condition. In particular, ICAC achieves system capacity higher than the PSIR-CAC and MCAC by more than 10% in traffic ranges where the QoS requirements are kept. ICAC is more adaptive and stable than the PSIR-CAC and MCAC.

The rest of the chapter is organized as follows. Section 3.3 describes the system model of a wideband CDMA cellular system and functional blocks within ICAC. Section 3.4 gives the designs for the fuzzy equivalent capacity estimator, the PRNN interference predictor, and the fuzzy call admission processor contained in ICAC. Simulation results and discussions are presented in section 3.5. Finally, conclusions are remarked in section 3.6.

3.3 System Model

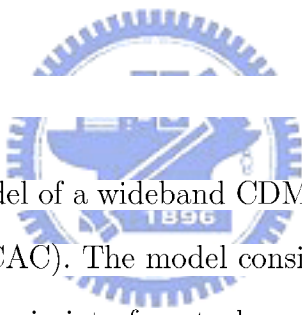


Fig. 3.1 depicts the system model of a wideband CDMA cellular system with the intelligent call admission controller (ICAC). The model considers K cells, where mobile users communicate with each other via air interface to base station (BS), and BSs are connected to a base station controller (BSC) or a radio network controller (RNC) containing the ICAC. The air interface adopts WCDMA protocol, and time in the air interface is divided into frames with duration T .

Input traffic generated within mobile users is categorized as real-time voice (type-1) and non-real-time data (type-2). New voice and data calls arrive at the system according to Poisson distributions with average arrival rates of λ_v and λ_d , respectively. Herein, the voice source is characterized by a two-state discrete-time Markov chain traffic model and generates an air-interface packet in each frame duration of T during ON state (talkspurt) but none during OFF state (silence). The mean durations of talkspurt and silence periods are assumed to be exponentially distributed with $1/\alpha$ and $1/\beta$, respectively. The data

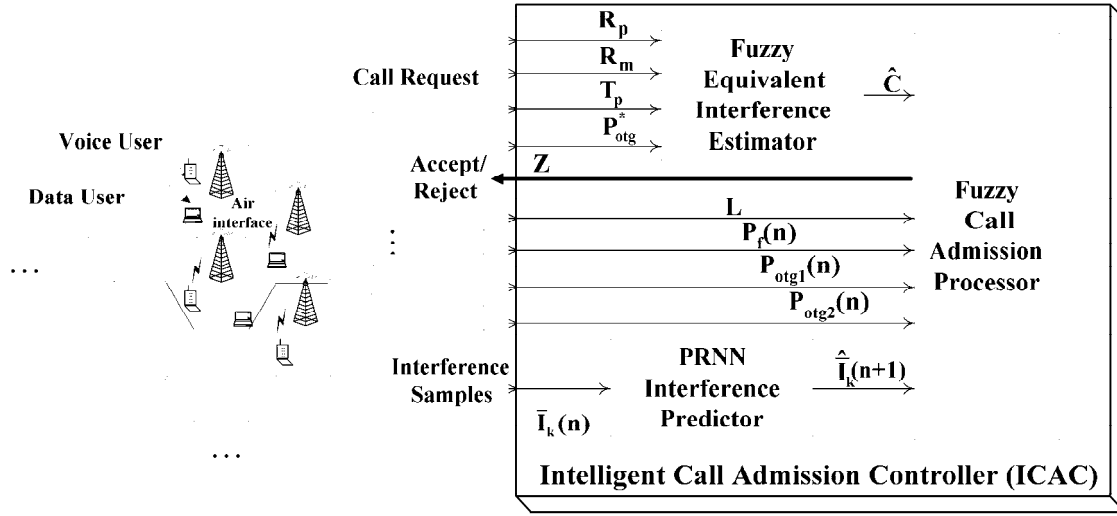


Figure 3.1: System model.

source is characterized by a batch Poisson process with an average message arrival rate of A_d . The size of data message is assumed to be a positive-valued random variable which is generally distributed. The data message will further be segmented into a number of air-interface packets according to the processing gain set for the service. Each terminal supports two finite separate buffers for voice and data services.

For differentiated bit-error-rate (BER) requirements set for the type-1 and the type-2 traffic, we define their individual processing gains, denoted by SF_1 and SF_2 . The SF_1 and SF_2 are chosen to be the closest integer greater than the required spreading factor. Corresponding to each specific BER requirement and processing gain, the signal to interference ratio (SIR) threshold values of type-1 and type-2 traffic, denoted by SIR_1^* and SIR_2^* , can be obtained. Two basic transmission rates (basic channels) are supported: (a) $R_1 = R$, which is dedicated to active voice users and is equal to the voice coding rate, and (b) $R_2 = R \cdot SF_1/SF_2$, which is dedicated to active data users. If a data user requires a transmission rate X higher than the basic transmission rate R_2 , this rate will be quantized into M times of R_2 , where $M = \lceil \frac{X}{R_2} \rceil$ and $\lceil \cdot \rceil$ denotes the smallest integer

greater than or equal to the argument, and each R_2 is encoded with a different pseudo-noise (PN) code. Under this circumstance, the data connection transmits with M basic channels ($M \geq 1$) simultaneously for communications, and the total transmission power is M times to the power of single code channel.

Assume that the number of PN codes available for code-division multiplexing is sufficiently large to support all services. A newly user determines its home cell to be the cell from which the pilot strength is the strongest. Mobile users are assumed to be uniformly distributed within the cell. When the user detects the pilot strength of another cell stronger than that of original cell by φ dB, the handoff procedure is performed.

In the radio propagation, the significant loss is assumed to contain the path loss and the shadowing. The short-term fading is averaged out by a window to form the interference measurement samples, and thus we here ignore the effect of short-term fading for the CAC. The generally accepted radio propagation (link gain) model, $L(r)$, is then the product of the θ th power of the distance and a correlated shadowing random variable $\zeta(r)$ of log-normal distribution with standard deviation σ_0 dB [6], which is given by

$$L(r) = 10^{\frac{\zeta}{10}} r^{-\theta}, \quad (3.1)$$

where r is the distance between the mobile user and the base station. The auto-correlation function for the fluctuation of shadow fading is assumed to be exponential, and is given by

$$E[\zeta(r_1)\zeta(r_2)] = \sigma_0^2 e^{-(r_1-r_2)/r_0}, \quad (3.2)$$

where r_0 denotes the decay of the correlation [60]. All users in their home cell are assumed to be perfectly power-controlled. Hence, the power level of a basic channel for either voice or data traffic received at base station equals a constant value S .

The received power at base station contains the desired user power and the interference power. At time instant n , the interference power in cell k , $1 \leq k \leq K$, denoted by

$I_k(n)$, consists of the home-cell interference, adjacent-cell interference, and additive white Gaussian noise, denoted by $I_{H,k}(n)$, $I_{A,k}(n)$, and η , respectively. That is, $I_k(n) = I_{H,k}(n) + I_{A,k}(n) + \eta$.

If there are $N_{1,k}$ type-1 users and $N_{2,k}$ type-2 users excluding the considered user in cell k , $I_{H,k}(n)$ is given by

$$I_{H,k}(n) = S \left[\sum_{i=1}^{N_{1,k}} \nu_{i,k} + \sum_{i=1}^{N_{2,k}} \delta_{i,k} \cdot M_{i,k}(n) \right], \quad (3.3)$$

where $\nu_{i,k}$ ($\delta_{i,k}$) denotes the type-1 (type-2) traffic activity factor, and $M_{i,k}(n)$ is the number of basic code channels needed by type-2 user i in home cell k for communication [9]. $I_{H,k}(n)$ is the same regardless of what the considered user is a type-1 user or a type-2 user. The adjacent-cell interference $I_{A,k}(n)$ which considers only the first-tier is given by

$$I_{A,k}(n) = S \sum_b \left[\sum_{i=1}^{N_{1,b}} \nu_{i,b} \cdot \left(\frac{r_{ib}}{r_{ik}}\right)^\theta \cdot 10^{(\zeta_{ik} - \zeta_{ib})/10} + \sum_{i=1}^{N_{2,b}} \delta_{i,b} \cdot M_{i,b}(n) \left(\frac{r_{ib}}{r_{ik}}\right)^\theta \cdot 10^{(\zeta_{ik} - \zeta_{ib})/10} \right], \quad (3.4)$$

where $b \in \{\text{the first-tier adjacent cells corresponding to cell } k\}$, r_{ik} is the distance of the user i in cell b to the base station of cell k , and r_{ib} is the distance of the user i in cell b to the base station of cell b . Consequently, the measured $SIR_k(n)$ at time n in BS k for each code channel of the considered voice or data users is given by

$$SIR_k(n) = \frac{S}{I_k(n)}. \quad (3.5)$$

As shown in Fig. 1, the proposed *intelligent call admission controller* (ICAC), mainly consists of a fuzzy equivalent interference estimator, PRNN interference predictor, and fuzzy call admission processor. The *fuzzy equivalent interference estimator* estimates the equivalent interference of a call request, denoted as \hat{C} , from its claimed traffic parameters: peak rate R_p , mean rate R_m , peak rate duration T_p , and its outage probability requirement P_{otg}^* . The *PRNN interference predictor* takes the interference mean at the present time

instant n , $\bar{I}_k(n)$, as an input variable to accurately predict the interference mean at the next time instant $(n + 1)$, $\hat{I}_k(n + 1)$. The $\bar{I}_k(n)$ is obtained by

$$I_k(n) = \frac{\sum_{j=0}^{N-1} I_k(n - jT)}{N}, \quad (3.6)$$

where N is the size of time window. And the *fuzzy call admission processor* chooses the forced termination probability for handoffs measured at present time n , denoted by $P_f(n)$, the outage probabilities of type-1 and type-2 services measured at the present time n , denoted by $P_{otg1}(n)$ and $P_{otg2}(n)$, $\hat{I}_k(n + 1)$, the link gain L in (3.1), and \hat{C} as input variables to determine the acceptance for the call request. Note that $P_{otgi}(n)$, $i = 1$ or 2 , is defined as

$$P_{otgi}(n) = Pr\{SIR_k(n) < SIR_i^*\}. \quad (3.7)$$

In the chapter, the required outage probability for type- i traffic, denoted by P_{otgi}^* , is set to be the system QoS requirements, instead of SIR_i^* . Furthermore, in order to protect the handoff connection against forced termination, the required probability of forced termination, denoted by P_f^* , is also set to be the QoS requirement. These system QoS performance measures such as $P_f(n)$, $P_{otg1}(n)$, and $P_{otg2}(n)$ act as a metric to reflect system performance and play as feedback signals for ICAC. Consequently, ICAC is a closed-loop control system in which system stability can be ensured and QoS requirements can be satisfied.

3.4 Intelligent Call Admission Controller

3.4.1 Fuzzy Equivalent Interference Estimator

Assume there is a call request with traffic parameters: the peak rate R_p , the mean rate R_m , the peak rate duration T_p , and the required outage probability P_{otg1}^* (P_{otg2}^*), in the cell k . Similar to the effective bandwidth method used in high-speed networks [4], [5], the

equivalent interference of call request (type-1 or type-2), denoted by \hat{C} (\hat{C}_1 for type-1, \hat{C}_2 for type-2) can be obtained by Gaussian approximation given in section 2.3.

Since the fuzzy approach exhibits a soft behavior that means having a great ability to deal with the real-world imprecise, uncertain traffic, we here adopt fuzzy implementation of the *fuzzy equivalent interference estimator*. The equivalent interference estimator takes R_p , R_m , T_p , and P_{otg}^* , claimed by a call request, as four input linguistic variables. The link gain variable is not considered here, but considered in the *fuzzy call admission processor*. This is because in this chapter, equal received power control is assumed, and the link gain variable affects only the adjacent cell interference but not the home cell interference.

Based on the knowledge obtained from the numerical results of above derivations, the design of the *fuzzy equivalent interference estimator* is as follows [62]. Term sets for R_p , R_m , T_p , and P_{otg}^* are defined as $T(R_p)=\{\text{Small, Medium, Large}\}=\{Sm, Me, La\}$, $T(R_m)=\{\text{Low, High}\}=\{Lo, Hi\}$, $T(T_p)=\{\text{Short, Middle, Long}\}=\{Sh, Md, Lg\}$, and $T(P_{otg}^*)=\{\text{Strict, Loose}\}=\{St, Ls\}$, respectively. Triangular function $f(x; x_0, a_0, a_1)$ and trapezoidal function $h(x; x_0, x_1, a_0, a_1)$ are chosen to be the membership functions, where x_0 in $f(\cdot)$ is the center of the triangular function, x_0 (x_1) in $h(\cdot)$ is the left (right) edge of the trapezoidal function, and a_0 (a_1) is the left (right) width of the triangular or the trapezoidal function.

Membership functions for $T(R_p)$, $T(R_m)$, $T(T_p)$, and $T(P_{otg}^*)$ are denoted by $M(R_p) = \{\mu_{Sm}, \mu_{Me}, \mu_{La}\}$, $M(R_m) = \{\mu_{Lo}, \mu_{Hi}\}$, $M(T_p) = \{\mu_{Sh}, \mu_{Md}, \mu_{Lg}\}$, and $M(P_{otg}^*) = \{\mu_{St}, \mu_{Ls}\}$, which are defined as

$$\mu_{Sm}(R_p) = h(\log(R_p); \log(R_{p,min}), Sm_e, 0, Sm_w), \quad (3.8)$$

$$\mu_{Me}(R_p) = f(\log(R_p); Me_c, Me_{w0}, Me_{w1}), \quad (3.9)$$

$$\mu_{La}(R_p) = h(\log(R_p); La_e, \log(R_{p,max}), La_w, 0), \quad (3.10)$$

$$\mu_{Lo}(R_m) = h\left(\frac{R_m}{R_p}; 0, Lo_w, 0, Lo_e\right), \quad (3.11)$$

$$\mu_{Hi}(R_m) = h\left(\frac{R_m}{R_p}\right); Hi_e, 1, Hi_w, 0), \quad (3.12)$$

$$\mu_{Sh}(T_p) = h(\log(T_p); \log(T_{p,min}), Sh_e, 0, Sh_w), \quad (3.13)$$

$$\mu_{Me}(T_p) = f(\log(T_p); Md_c, Md_{w0}, Md_{w1}), \quad (3.14)$$

$$\mu_{Lg}(T_p) = h(\log(T_p); Lg_e, \log(T_{p,max}), Lg_w, 0), \quad (3.15)$$

$$\mu_{St}(P_{otg}^*) = f(\log P_{otg}^*; \log P_{otg2}^*, S1, S0), \quad (3.16)$$

$$\mu_{Ls}(P_{otg}^*) = f(\log P_{otg}^*; \log P_{otg1}^*, S0, S1), \quad (3.17)$$

where $R_{p,min}$, $R_{p,max}$, $T_{p,min}$, and $T_{p,max}$, are the minimum and the maximum possible values for R_p and T_p , respectively; P_{otg1}^* and P_{otg2}^* are the desired QoS requirements of outage probability for type-1 and type-2 traffic; $S0$ and $S1$ are the two boundaries for the membership function of $\mu_{Ls}(P_{otg}^*)$ and $\mu_{St}(P_{otg}^*)$ such that these two membership function are mutually mirrored. Since R_p , T_p , and P_{otg}^* vary widely from different traffic sources, a logarithm function is employed. According to numerical results, proper boundary values of the membership functions are set to characterize R_p , R_m , and T_p . Also, $Sm_w = Me_{w0} = Me_c - Sm_e$, $La_w = Me_{w1} = La_e - Me_c$, $Lo_w = Hi_w = Hi_e - Lo_e$, $Sh_w = Md_{w0} = Md_c - Sh_e$, and $Lg_w = Md_{w1} = Lg_e - Md_c$ are set and fine-tuned. The output linguistic variable is the equivalent interference \hat{C} (\hat{C}_1 or \hat{C}_2); its term set is defined as $T(\hat{C}) = \{C_1, C_2, C_3, C_4, C_5, C_6, C_7, C_8\}$. The membership function of $T(\hat{C})$ is denoted by $M(\hat{C}) = \{\mu_{C_1}, \mu_{C_2}, \mu_{C_3}, \mu_{C_4}, \mu_{C_5}, \mu_{C_6}, \mu_{C_7}, \mu_{C_8}\}$, where

$$\mu_{C_1}(\hat{C}) = f(\hat{C}; C_{1,c}, 0, 0), \quad (3.18)$$

$$\mu_{C_2}(\hat{C}) = f(\hat{C}; C_{2,c}, 0, 0), \quad (3.19)$$

$$\mu_{C_3}(\hat{C}) = f(\hat{C}; C_{3,c}, 0, 0), \quad (3.20)$$

$$\mu_{C_4}(\hat{C}) = f(\hat{C}; C_{4,c}, 0, 0), \quad (3.21)$$

$$\mu_{C_5}(\hat{C}) = f(\hat{C}; C_{5,c}, 0, 0), \quad (3.22)$$

$$\mu_{C_6}(\hat{C}) = f(\hat{C}; C_{6,e}, 0, 0), \quad (3.23)$$

$$\mu_{C_7}(\hat{C}) = f(\hat{C}; C_{7,e}, 0, 0), \quad (3.24)$$

$$\mu_{C_8}(\hat{C}) = f(\hat{C}; C_{8,e}, 0, 0), \quad (3.25)$$

where $C_{1,e} = R_m$ and $C_{i,e} = C_{i-1,e} + \frac{R_p - R_m}{7}$, $i = 2, \dots, 8$.

According to the fuzzy set theory, the fuzzy rule base forms a fuzzy set with dimensions $|T(R_p)| \times |T(R_m)| \times |T(T_p)| \times |T(P_{otg}^*)|$ ($|T(x)|$ denotes the number of terms in $T(x)$). Therefore, there are a total of thirty six fuzzy inference rules. Table 3.2 lists these fuzzy inference rules, which are set based on knowledge described by examples as follows. In rule 31, rule 32, and rule 35, the peak rate is large and the mean rate is high. The resulting interference in rule 31, which has a short peak rate duration, is thus expected to be less than that in rule 35, which has a long peak rate duration. And rule 31, which has a loose QoS requirements, is considered to have lower resulting interference than rule 35, which has a strict QoS requirement.

In the inference process, the *max-min* inference method is adopted. The *max-min* inference method initially applies the *min* operator on membership values of terms of all input linguistic variables for each rule and then applies the *max* operator to yield the overall membership value, for each output term. For example, there are rule 2, rule 4, rule 6, rule 7, and rule 14 which have the same term C_2 . Results of the *min* operator for rule 2, rule 4, rule 6, rule 7, and rule 14, denoted as w_2, w_4, w_6, w_7 , and w_{14} , are expressed as

$$w_2 = \min(\mu_{Sm}(R_p), \mu_{Lo}(R_m), \mu_{Sh}(T_p), \mu_{St}(P_{otg}^*)), \quad (3.26)$$

$$w_4 = \min(\mu_{Sm}(R_p), \mu_{Lo}(R_m), \mu_{Md}(T_p), \mu_{St}(P_{otg}^*)), \quad (3.27)$$

$$w_6 = \min(\mu_{Sm}(R_p), \mu_{Hi}(R_m), \mu_{Lg}(T_p), \mu_{St}(P_{otg}^*)), \quad (3.28)$$

$$w_7 = \min(\mu_{Sm}(R_p), \mu_{Hi}(R_m), \mu_{Sh}(T_p), \mu_{Ls}(P_{otg}^*)), \quad (3.29)$$

$$w_{14} = \min(\mu_{Me}(R_p), \mu_{Lo}(R_m), \mu_{Sh}(T_p), \mu_{St}(P_{otg}^*)), \quad (3.30)$$

Then, the result after the *max* operator, for the term C_2 , denoted as w_{C_2} , can be obtained by

$$w_{C_2} = \max(w_2, w_4, w_6, w_7, w_{14}). \quad (3.31)$$

The center of area defuzzification method is used for the defuzzifier owing to its computational simplicity. This defuzzification method obtains the equivalent interference \hat{C} by combining $w_{C_1}, w_{C_2}, w_{C_3}, w_{C_4}, w_{C_5}, w_{C_6}, w_{C_7}$, and w_{C_8} as

$$\hat{C} = \frac{\sum_{i=1}^8 w_{C_i} \times C_{i,e}}{\sum_{i=1}^8 w_{C_i}}. \quad (3.32)$$

Table 3.2: Rule structure for the fuzzy capacity requirement estimator.

Rule	R_p	R_m	T_p	P_{otg}^*	\hat{C}	Rule	R_p	R_m	T_p	P_{otg}^*	\hat{C}
1	<i>Sm</i>	<i>Lo</i>	<i>Sh</i>	<i>Ls</i>	C_1	19	<i>Me</i>	<i>Hi</i>	<i>Sh</i>	<i>Ls</i>	C_4
2	<i>Sm</i>	<i>Lo</i>	<i>Sh</i>	<i>St</i>	C_2	20	<i>Me</i>	<i>Hi</i>	<i>Sh</i>	<i>St</i>	C_5
3	<i>Sm</i>	<i>Lo</i>	<i>Md</i>	<i>Ls</i>	C_1	21	<i>Me</i>	<i>Hi</i>	<i>Md</i>	<i>Ls</i>	C_5
4	<i>Sm</i>	<i>Lo</i>	<i>Md</i>	<i>St</i>	C_2	22	<i>Me</i>	<i>Hi</i>	<i>Md</i>	<i>St</i>	C_6
5	<i>Sm</i>	<i>Lo</i>	<i>Lg</i>	<i>Ls</i>	C_1	23	<i>Me</i>	<i>Hi</i>	<i>Lg</i>	<i>Ls</i>	C_5
6	<i>Sm</i>	<i>Lo</i>	<i>Lg</i>	<i>St</i>	C_2	24	<i>Me</i>	<i>Hi</i>	<i>Lg</i>	<i>St</i>	C_7
7	<i>Sm</i>	<i>Hi</i>	<i>Sh</i>	<i>Ls</i>	C_2	25	<i>La</i>	<i>Lo</i>	<i>Sh</i>	<i>Ls</i>	C_3
8	<i>Sm</i>	<i>Hi</i>	<i>Sh</i>	<i>St</i>	C_3	26	<i>La</i>	<i>Lo</i>	<i>Sh</i>	<i>St</i>	C_4
9	<i>Sm</i>	<i>Hi</i>	<i>Md</i>	<i>Ls</i>	C_3	27	<i>La</i>	<i>Lo</i>	<i>Md</i>	<i>Ls</i>	C_5
10	<i>Sm</i>	<i>Hi</i>	<i>Md</i>	<i>St</i>	C_4	28	<i>La</i>	<i>Lo</i>	<i>Md</i>	<i>St</i>	C_6
11	<i>Sm</i>	<i>Hi</i>	<i>Lg</i>	<i>Ls</i>	C_3	29	<i>La</i>	<i>Lo</i>	<i>Lg</i>	<i>Ls</i>	C_6
12	<i>Sm</i>	<i>Hi</i>	<i>Lg</i>	<i>St</i>	C_4	30	<i>La</i>	<i>Lo</i>	<i>Lg</i>	<i>St</i>	C_7
13	<i>Me</i>	<i>Lo</i>	<i>Sh</i>	<i>Ls</i>	C_1	31	<i>La</i>	<i>Hi</i>	<i>Sh</i>	<i>Ls</i>	C_6
14	<i>Me</i>	<i>Lo</i>	<i>Sh</i>	<i>St</i>	C_2	32	<i>La</i>	<i>Hi</i>	<i>Sh</i>	<i>St</i>	C_7
15	<i>Me</i>	<i>Lo</i>	<i>Md</i>	<i>Ls</i>	C_3	33	<i>La</i>	<i>Hi</i>	<i>Md</i>	<i>Ls</i>	C_7
16	<i>Me</i>	<i>Lo</i>	<i>Md</i>	<i>St</i>	C_4	34	<i>La</i>	<i>Hi</i>	<i>Md</i>	<i>St</i>	C_8
17	<i>Me</i>	<i>Lo</i>	<i>Lg</i>	<i>Ls</i>	C_4	35	<i>La</i>	<i>Hi</i>	<i>Lg</i>	<i>Ls</i>	C_8
18	<i>Me</i>	<i>Lo</i>	<i>Lg</i>	<i>St</i>	C_5	36	<i>La</i>	<i>Hi</i>	<i>Lg</i>	<i>St</i>	C_8

3.4.2 PRNN Interference Predictor

Since the neural networks have the learning capability and can dynamically adjust connection weights to achieve optimality for prediction, we here adopt the neural networks to obtain the existing-call interference of one-step further. The interference process is assumed to be in a non-linear auto-regressive moving average (NARMA) model. Approximating the NARMA model in the least mean square error sense allows us to express the one-step prediction of the mean interference as a function of p measured interference powers and q previously predicted interference powers. That is,

$$\hat{I}_k(n+1) = H(\bar{I}_k(n), \dots, \bar{I}_k(n-p+1); \hat{I}_k(n), \dots, \hat{I}_k(n-q+1)), \quad (3.33)$$

where $\hat{I}_k(i)$ is the previously predicted mean interference sample at time i , $n-q+1 \leq i \leq n$, in cell k , $\bar{I}_k(i)$ is the measured mean interference sample at time i , $n-p+1 \leq i \leq n$, and $H(\cdot)$ is an unknown nonlinear function to be determined. Applying *pipeline recurrent neural network* (PRNN) to the NARMA prediction yields a high prediction accuracy, fast convergent speed, and low computation complexity [65]. Thus, PRNN is adopted herein to approximate the $H(\cdot)$ function.

Fig. 3.2 shows the architecture of PRNN interference predictor, which involves a total of q levels of processing. Each level has an identical neural module and a subtractor. For level i , two external inputs are fed into the module: the delayed version of the measured interference sample $\bar{I}_k(n-i+1)$ and the first output of the preceding level $y_{i+1,1}(n)$, and the output of this module subtracted from $\bar{I}_k(n-i+2)$ forms an error signal $e_i(n)$. The error signal is used to adjust the synaptic weights in the i th neural module. Consequently, the output of the first module $y_{1,1}(n)$ is the desired next-step interference prediction $\hat{I}_s(n+1)$.

Fig. 3.3 depicts the detailed structure of module i , which is constituted by a two-layer recurrent neural network. The output vector, $\vec{y}_i(n) = [y_{i,1}(n), \dots, y_{i,M}(n)]$, consists of M elements, among which, $(M-1)$ outputs are fed back to the input, and the first output,

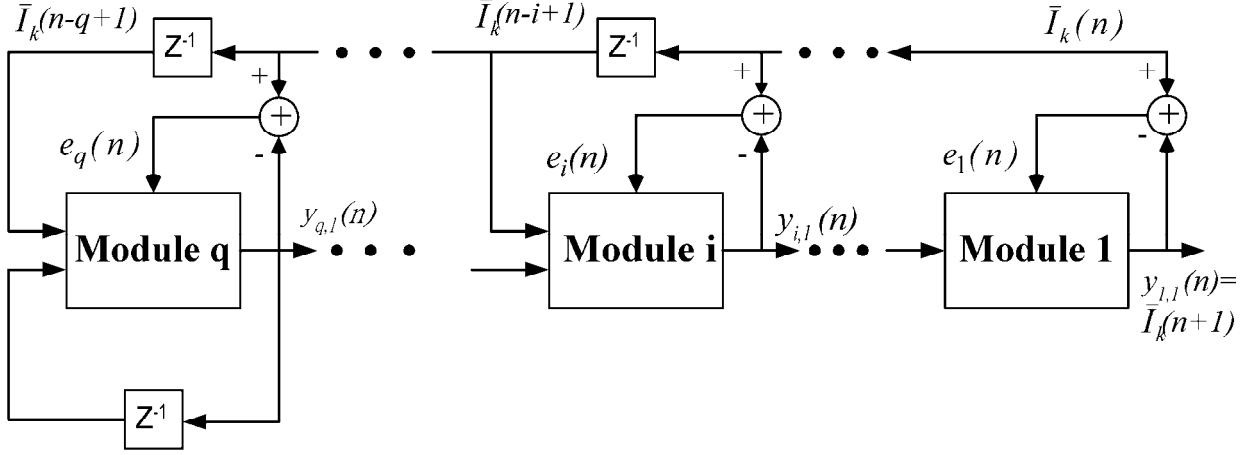


Figure 3.2: Structure of the PRNN interference predictor.

$y_{i,1}(n)$, is applied directly to the next module $i - 1$. The input vector $\vec{u}_i(n)$ consists of three parts: the p -tuple external input vector, $[\hat{I}_k(n - i + 1), \dots, \hat{I}_k(n - i - p + 2)]$, a bias input whose value is always maintained at $+1$, a feedforward input from the preceding level, $y_{i+1,1}(n)$, and the M -tuple feedback vector, $[y_{i,2}(n - 1), \dots, y_{i,M}(n - 1)]$. The details can be referred to [63], [64], [65].

To adjust the synaptic weights, we define a cost function based on these error signals, which is given by

$$\mathcal{E}(n) = \sum_{i=1}^q \lambda^{i-1} e_i^2(n), \quad (3.34)$$

where λ is an exponential weighting factor of the range $(0 < \lambda \leq 1)$ [63]. The factor λ^{i-1} weighs the memory of module i in the PRNN. Notably, $e_i(n) = \bar{I}_k(n - i + 2) - y_{i,1}(n)$. Because $y_{i,1}(n)$ is limited in amplitude within the range $(0,1)$ due to the characteristics of sigmoidal activation function, $\bar{I}_k(n - i + 2)$ is normalized before being actually put into the PRNN predictor.

The synaptic weights are adjusted by using a RTRL algorithm [64], [65]. For a synaptic weight $w_{\zeta,\xi}$, the incremental change $\Delta w_{\zeta,\xi}(n)$ at time n according to the steepest descent

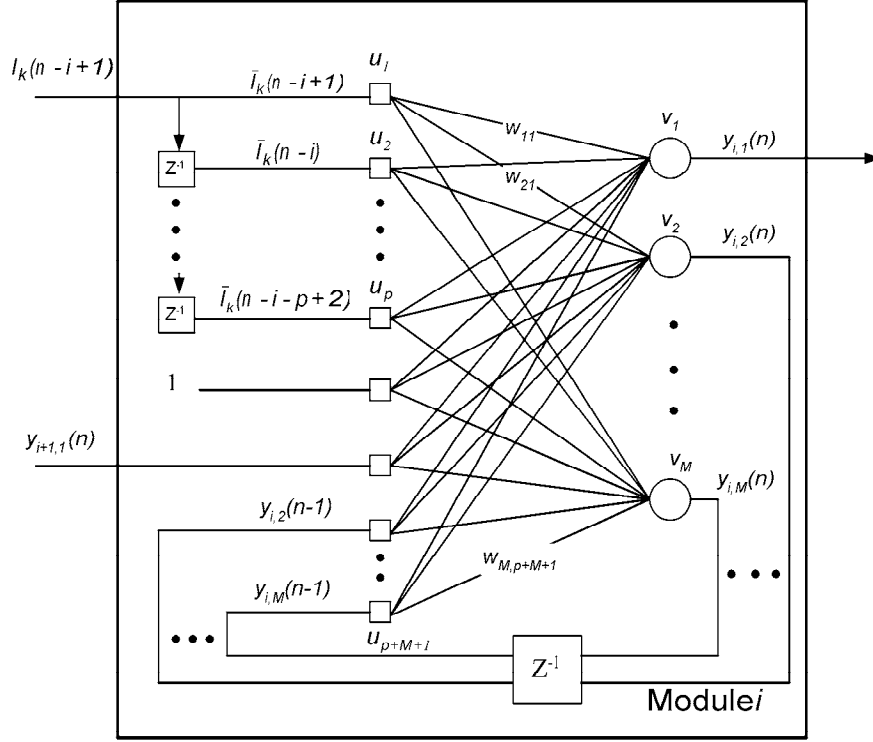


Figure 3.3: The i th small RNN module in the PRNN interference predictor.

method is expressed as

$$\begin{aligned} \Delta w_{\zeta,\xi}(n) &= -\eta \frac{\partial \mathcal{E}(n)}{\partial w_{\zeta,\xi}}, \\ &= 2\eta \sum_{i=1}^q \lambda^{i-1} e_i(n) \cdot \frac{\partial y_{i,1}(n)}{\partial w_{\zeta,\xi}}. \end{aligned} \quad (3.35)$$

The PRNN interference predictor obtains the interference predictions for existing calls at time instant $(n+1)$, $\hat{I}_k(n+1)$, from the output of the first neuron of the first module. Notably, the computation of a PRNN prediction is proportional to $q \times M^4 = M^4/q^3$. Thus, PRNN is much faster than RNN.

3.4.3 Fuzzy Call Admission Processor

The *fuzzy call admission processor* is responsible for the determination of the acceptance of a new or handoff call request. For the new call request, the processor considers the P_f ,

P_{otg1} , P_{otg2} , $\bar{I}_s(n+1)$, L , and \hat{C} as its input linguistic variables which indicate the system performance measures, the predicted system load, the link quality, and the estimated equivalent interference generated by the call. For the handoff call request, the processor considers the same input variable as for the new call request except that the link quality L is not taken into account since the handoff call is definitely on the cell boundary.

According to the domain knowledge from simulations, term sets of these input linguistic variables are set to be $T(P_f)=\{\text{Satisfied, Not Satisfied}\}=\{Sa_f, Ns_f\}$, $T(P_{otg1})=\{\text{Satisfied, Not Satisfied}\}=\{Sa1, Ns1\}$, $T(P_{otg2})=\{\text{Satisfied, Not Satisfied}\}=\{Sa2, Ns2\}$, $T(\hat{I}_{n+1})=\{\text{Small, Large}\}=\{Sm, Lg\}$, $T(L)=\{\text{Strong, Weak}\}=\{Sr, Wk\}$, and $T(\hat{C})=\{\text{Small, Large}\}=\{Sc, Lc\}$. The term set for the output linguistic variable for new call request $Z = Z_n$ is $T(Z_n)=\{\text{Straightly Accept, Weakly Accept, Weakly Reject, Straightly Reject}\}=\{SA_n, WA_n, WR_n, SR_n\}$, and $Z = Z_h$ for the handoff call request is $T(Z_h)=\{\text{Straightly Accept, Weakly Accept, Weakly Reject, Straightly Reject}\}=\{SA_h, WA_h, WR_h, SR_h\}$.

Membership functions for the input linguistic variables are denoted by $M(P_f) = \{\mu_{Sa_f}, \mu_{Ns_f}\}$, $M(P_{otg1}) = \{\mu_{Sa1}, \mu_{Ns1}\}$, $M(P_{otg2}) = \{\mu_{Sa2}, \mu_{Ns2}\}$, $M(\hat{I}_s(n+1)) = \{\mu_{Sm}, \mu_{Lg}\}$, $M(L) = \{\mu_{Sr}, \mu_{Wk}\}$, and $M(\hat{C}) = \{\mu_{Sc}, \mu_{Lc}\}$, where

$$\mu_{Sa_f}(P_f(n)) = h(P_f(n); 0, Sa_{ef}, 0, Sa_{wf}), \quad (3.36)$$

$$\mu_{Ns_f}(P_f(n)) = h(P_f(n); Ns_{ef}, 1, Ns_{wf}, 0), \quad (3.37)$$

$$\mu_{Sa1}(P_{otg1}(n)) = h(P_{otg1}(n); 0, Sa_{e1}, 0, Sa_{w1}), \quad (3.38)$$

$$\mu_{Ns1}(P_{otg1}(n)) = h(P_{otg1}(n); Ns_{e1}, 1, Ns_{w1}, 0), \quad (3.39)$$

$$\mu_{Sa2}(P_{otg2}(n)) = h(P_{otg2}(n); 0, Sa_{e2}, 0, Sa_{w2}), \quad (3.40)$$

$$\mu_{Ns2}(P_{otg2}(n)) = h(P_{otg2}(n); Ns_{e2}, 1, Ns_{w2}, 0), \quad (3.41)$$

$$\mu_{Sm}(\hat{I}_k(n+1)) = h(\hat{I}_k(n+1); 0, Sm_e, 0, Sm_w), \quad (3.42)$$

$$\mu_{Lg}(\hat{I}_k(n+1)) = h(\hat{I}_k(n+1); I_o, \infty, Lg_w, 0), \quad (3.43)$$

$$\mu_{Sr}(L) = h(L/L_0; 0, Sr_e, 0, Sr_w), \quad (3.44)$$

$$\mu_{Wk}(L) = h(L/L_0; Wk_e, \infty, Wk_w, 0), \quad (3.45)$$

$$\mu_{Sc}(\hat{C}) = h(\hat{C}; 0, Sc_e, 0, Sc_w), \quad (3.46)$$

$$\mu_{Lc}(\hat{C}) = h(\hat{C}; Lc_e, Lc_{e1}, Lc_w, 0), \quad (3.47)$$

where $N_{S_{ef}}$ is set to be P_f^* minus a safety margin, and Sa_{ef} is a value less than $N_{S_{ef}}$ by a safety amount for separating the satisfactory region and the violation region; $N_{S_{e1}}$ ($N_{S_{e2}}$) is set to be P_{otg1}^* (P_{otg2}^*) minus a safety margin, and Sa_{e1} (Sa_{e2}) is also set to a value less than $N_{S_{e1}}$ ($N_{S_{e2}}$) for the same reason as the safety amount for Sa_{ef} ; I_o is the tolerable interference power corresponding to the minimal signal-to-interference power ratio SIR_1^* , and Sm_e would be set to be a fraction of I_o ; L_0 is the reference link gain within which the mobile user is regarded as to be far from the base station and the interference to the adjacent cells is greater, and $Sr_e \geq 1$ and $Wk_e \leq 1$. We also set $Sc_w = Lc_w = Lc_e - Sc_e$, $Sm_w = I_o - Sm_e = Lg_w$ to simplify the design of fuzzy logic parameters. The other endpoints of Sc_e , Lc_e , Lc_{e1} , and the widths of the membership function of Sa_{wf} , $N_{S_{wf}}$, Sa_{w1} , $N_{S_{w1}}$, Sa_{w2} , $N_{S_{w2}}$, Sr_w , and Wk_w must be fine-tuned to proper values during simulations.

Membership functions for the output linguistic variable of new call request are denoted by $M(Z_n) = \{\mu_{SA_n}, \mu_{WA_n}, \mu_{WR_n}, \mu_{SR_n}\}$, where

$$\mu_{SA_n}(Z_n) = f(Z_n; SA_n, 0, 0), \quad (3.48)$$

$$\mu_{WA_n}(Z_n) = f(Z_n; WA_n, 0, 0), \quad (3.49)$$

$$\mu_{WR_n}(Z_n) = f(Z_n; WR_n, 0, 0), \quad (3.50)$$

$$\mu_{SR_n}(Z_n) = f(Z_n; SR_n, 0, 0). \quad (3.51)$$

A new call request can be accepted if the output of the fuzzy call admission processor

Table 3.3: Rule structure of the fuzzy call admission processor for the new call request.

Rule	P_f	P_{otg1}	P_{otg2}	\hat{I}_{n+1}	L	\hat{C}	Z_n
1	Sa_h	$Sa1$	$Sa2$	Sm	-	-	SA_n
2	Sa_h	$Sa1$	$Sa2$	Lg	Sr	Sc	SA_n
3	Sa_h	$Sa1$	$Sa2$	Lg	Sr	Lc	WA_n
4	Sa_h	$Sa1$	$Sa2$	Lg	Wk	-	WR_n
5	Sa_h	$Sa1$	$Ns2$	Sm	Sr	Sc	SA_n
6	Sa_h	$Sa1$	$Ns2$	Sm	Sr	Lc	WA_n
7	Sa_h	$Sa1$	$Ns2$	Sm	Wk	Sc	WA_n
8	Sa_h	$Sa1$	$Ns2$	Sm	Wk	Lc	WR_n
9	Sa_h	$Sa1$	$Ns2$	Lg	Sr	Sc	WA_n
10	Sa_h	$Sa1$	$Ns2$	Lg	Sr	Lc	WR_n
11	Sa_h	$Sa1$	$Ns2$	Lg	Wk	Sc	WR_n
12	Sa_h	$Sa1$	$Ns2$	Lg	Wk	Lc	SR_n
13	Sa_h	$Ns1$	$Sa2$	Sm	Sr	Sc	WA_n
14	Sa_h	$Ns1$	$Sa2$	Sm	Sr	Lc	WR_n
15	Sa_h	$Ns1$	$Sa2$	Sm	Wk	Sc	WA_n
16	Sa_h	$Ns1$	$Sa2$	Sm	Wk	Lc	WR_n
17	Sa_h	$Ns1$	$Sa2$	Lg	Sr	-	WR_n
18	Sa_h	$Ns1$	$Sa2$	Lg	Wk	-	SR_n
19	Sa_h	$Ns1$	$Ns2$	Sm	Sr	Sc	WA_n
20	Sa_h	$Ns1$	$Ns2$	Sm	Sr	Lc	WR_n
21	Sa_h	$Ns1$	$Ns2$	Sm	Wk	-	SR_n
22	Sa_h	$Ns1$	$Ns2$	Lg	Sr	-	SR_n
23	Sa_h	$Ns1$	$Ns2$	Lg	Wk	-	SR_n
24	Na_h	$Sa1$	$Sa2$	Sm	-	-	WA_n
25	Na_h	$Sa1$	$Sa2$	Lg	Sr	-	WA_n
26	Na_h	$Sa1$	$Sa2$	Lg	Wk	-	WR_n

27	Na_h	$Sa1$	$Ns2$	Sm	Sr	-	WA_n
28	Na_h	$Sa1$	$Ns2$	Sm	Wk	Sc	WR_n
29	Na_h	$Sa1$	$Ns2$	Sm	Wk	Lc	SR_n
30	Na_h	$Sa1$	$Ns2$	Lg	Sr	Sc	WR_n
31	Na_h	$Sa1$	$Ns2$	Lg	Sr	Lc	SR_n
32	Na_h	$Sa1$	$Ns2$	Lg	Wk	-	SR_n
33	Na_h	$Ns1$	$Sa2$	Sm	Sr	-	WR_n
34	Na_h	$Ns1$	$Sa2$	Sm	Wk	Sc	WR_n
35	Na_h	$Ns1$	$Sa2$	Sm	Wk	Lc	SR_n
36	Na_h	$Ns1$	$Sa2$	Lg	-	-	SR_n
37	Na_h	$Ns1$	$Ns2$	-	-	-	SR_n

Z_n is greater than an acceptance threshold z_{na} , $SR_n \leq z_{na} \leq SA_n$. Without a loss of generality, $SR_n=0$, $SA_n=1$, and let $WR_n=(SR_n + z_{na})/2$, $WA_n=(SA_n + z_{na})/2$. And membership functions for the output linguistic variable of handoff call request are denoted by $M(Z_h) = \{\mu_{SA_h}, \mu_{WA_h}, \mu_{WR_h}, \mu_{SR_h}\}$, where

$$\mu_{SA_h}(Z_h) = f(Z_h; A_h, 0, 0), \quad (3.52)$$

$$\mu_{WA_h}(Z_h) = f(Z_h; WA_h, 0, 0), \quad (3.53)$$

$$\mu_{WR_h}(Z_h) = f(Z_h; WR_h, 0, 0), \quad (3.54)$$

$$\mu_{SR_h}(Z_h) = f(Z_h; R_h, 0, 0). \quad (3.55)$$

A handoff call request can be accepted if the output of the fuzzy call admission processor Z_h is greater than an acceptance threshold z_{ha} , $R_h \leq z_{ha} \leq A_h$. Similarly, we set $R_h=0$, $A_h=1$, $WR_h=(R_h + z_{ha})/2$, and $WA_h=(A_h + z_{ha})/2$.

Table 3.3 presents the rule structure of *fuzzy call admission processor* for the new call requests. Clearly, the more (less) satisfied the P_f , P_{otg1} , P_{otg2} and the smaller (larger) the \hat{I}_{n+1} , the higher (lower) likelihood that the system can accept the new call request. As P_f is not satisfied, but P_{otg1} , P_{otg2} , and \hat{I}_{n+1} indicate the light system load, the system will tend to accept the new call request to enhance the utilization since the relief from

Table 3.4: Rule structure of the fuzzy handoff admission processor for the handoff call request.

Rule	P_f	P_{otg1}	P_{otg2}	\hat{I}_{n+1}	\hat{C}	Z_h	Rule	P_f	P_{otg1}	P_{otg2}	\hat{I}_{n+1}	\hat{C}	Z_h
1	Sa_f	$Sa1$	$Sa2$	Sm	Sc	SA_h	17	Ns_f	$Sa1$	$Sa2$	Sm	Sc	SA_h
2	Sa_f	$Sa1$	$Sa2$	Sm	Lc	SA_h	18	Ns_f	$Sa1$	$Sa2$	Sm	Lc	SA_h
3	Sa_f	$Sa1$	$Sa2$	Lg	Sc	SA_h	19	Ns_f	$Sa1$	$Sa2$	Lg	Sc	SA_h
4	Sa_f	$Sa1$	$Sa2$	Lg	Lc	SA_h	20	Ns_f	$Sa1$	$Sa2$	Lg	Lc	SA_h
5	Sa_f	$Sa1$	$Ns2$	Sm	Sc	WA_h	21	Ns_f	$Sa1$	$Ns2$	Sm	Sc	SA_h
6	Sa_f	$Sa1$	$Ns2$	Sm	Lc	WR_h	22	Ns_f	$Sa1$	$Ns2$	Sm	Lc	SA_h
7	Sa_f	$Sa1$	$Ns2$	Lg	Sc	WR_h	23	Ns_f	$Sa1$	$Ns2$	Lg	Sc	WA_h
8	Sa_f	$Sa1$	$Ns2$	Lg	Lc	WR_h	24	Ns_f	$Sa1$	$Ns2$	Lg	Lc	WR_h
9	Sa_f	$Ns1$	$Sa2$	Sm	Sc	WR_h	25	Ns_f	$Ns1$	$Sa2$	Sm	Sc	SA_h
10	Sa_f	$Ns1$	$Sa2$	Sm	Lc	WR_h	26	Ns_f	$Ns1$	$Sa2$	Sm	Lc	SA_h
11	Sa_f	$Ns1$	$Sa2$	Lg	Sc	SR_h	27	Ns_f	$Ns1$	$Sa2$	Lg	Sc	WA_h
12	Sa_f	$Ns1$	$Sa2$	Lg	Lc	SR_h	28	Ns_f	$Ns1$	$Sa2$	Lg	Lc	WR_h
13	Sa_f	$Ns1$	$Ns2$	Sm	Sc	SR_h	29	Ns_f	$Ns1$	$Ns2$	Sm	Sc	SR_h
14	Sa_f	$Ns1$	$Ns2$	Sm	Lc	SR_h	30	Ns_f	$Ns1$	$Ns2$	Sm	Lc	SR_h
15	Sa_f	$Ns1$	$Ns2$	Lg	Sc	SR_h	31	Ns_f	$Ns1$	$Ns2$	Lg	Sc	SR_h
16	Sa_f	$Ns1$	$Ns2$	Lg	Lc	SR_h	32	Ns_f	$Ns1$	$Ns2$	Lg	Lc	SR_h

a temporary congestion may happen. At any specific system load condition, the system will tend to reject the bad users with poor signal quality and the more heavy loaded users according to L and \hat{C} .

Table 3.4 presents the rule structure of the fuzzy call admission processor for handoff call requests. It tends to accept the handoff call as the P_f is not satisfied more likely than as P_f is satisfied, in order to protect the on-going call anyway except the condition that the traffic load is very heavy. And the larger \hat{I}_{n+1} , P_{otg1} , and P_{otg2} imply the heavier traffic load, then the system tends to reject the handoff call request.

Similarly, the *max-min* inference method is employed herein to calculate the membership value for each term of $T(Z_n)$ ($T(Z_n)$) and the center of area method is then applied for defuzzification.

3.5 Simulation Results and Discussion

In the simulations, $K = 49$ hexagonal cells, frame time $T = 20$ ms, E_b over N_0 of type-1 connection $\gamma_1^* = 7dB$, E_b over N_0 of type-2 connection $\gamma_2^* = 10dB$, the spreading factor of each basic code channel $SF = 256$, and the frequency spectrum bandwidth $W = 3.8325$ MHz are selected. The QoS requirements of outage probability are set to be $P_{otg1}^* = 2 * 10^{-2}$ and $P_{otg2}^* = 5 * 10^{-3}$, and the QoS constraint of forced termination probability is defined as $P_f^* = 5 * 10^{-5}$. To achieve the required outage requirement of type-2 connections, the processing gain ratio is chosen to be $\frac{R_2}{R_1} = 3$, and therefore the SIR threshold before despreading are set to be $SIR_1^* = -14$ dB, $SIR_2^* = -17$ dB. The filtering factor (the exponential decay factor) to obtain the interference mean estimation is 0.02. The voice source model is assumed to be with $1/\alpha = 1$ second and $1/\beta = 1.35$ seconds, while the data source model is assumed to be with $1/A_d = 0.1$ and the size of data message is in a geometric distribution with mean 2 and maximum length 10. The mean holding times for both voice and data services are 90 seconds. The moving speed of each mobile user V has two simulation cases. In the low mobility case, the speed of a mobile user is randomly selected from $0Km/Hr$ or $5Km/Hr$. In the high mobility case, the speed of mobile users is either $V_1 = 20Km/Hr$ or $V_2 = 60Km/Hr$ with equal probability. The moving direction is modelled by the angle τ with uniform distribution. The radio propagation parameters of θ and ζ are set to be 4 and 8dB [6], and the handoff margin is set to be 3dB.

The effectiveness of the proposed ICAC is tested by comparing it with the SIR-based CAC with inter-cell interference prediction (PSIR-CAC) proposed in [14] and the CAC for multimedia calls (MCAC) proposed in [30]. For PSIR-CAC [14], the call request is accepted if the minimum residual capacity of each cell among the active sets is positive. The SIR threshold is set to be -14dB. For MCAC, E_b/N_0 threshold values for the type-1

and type-2 services, denoted by γ_0 and γ_1 , are set to be 7dB and 10dB, respectively. This algorithm accepts a call request of type i , $i = 1$ or 2 , if the condition for type k connection satisfies

$$\left(\left(\frac{E_b}{N_0} \right)_{k,i}^{-1} + \sum_{j=1}^{M_c} 1/SF_{i,j} \right)^{-1} \geq \gamma_k^* \cdot \beta_i^x, \quad k = 1, 2, \quad (3.56)$$

where β_i^x , $x = n$ or h for new or handoff call request, is the admission margin parameter to give different priorities for new or handoff call requests of type- i class, and $(E_b/N_0)_{k,i}$ is the measured mean E_b/N_0 of type k , M_c is the number of code channels, and $SF_{i,j}$ is the spreading factor of channel j for the call request of type i . We set $\beta_1^n = 1.25$, $\beta_2^n = 1.3$, $\beta_1^h = 1.05$, and $\beta_2^h = 1.1$. In the original scheme [30], single code and variable spreading factor transmission was used. Here we extend it to a multi-code transmission system, using the same design concept. Thus, $SF_{i,j}$ of each code is 256, but multi code channels are used to carry the information bits.

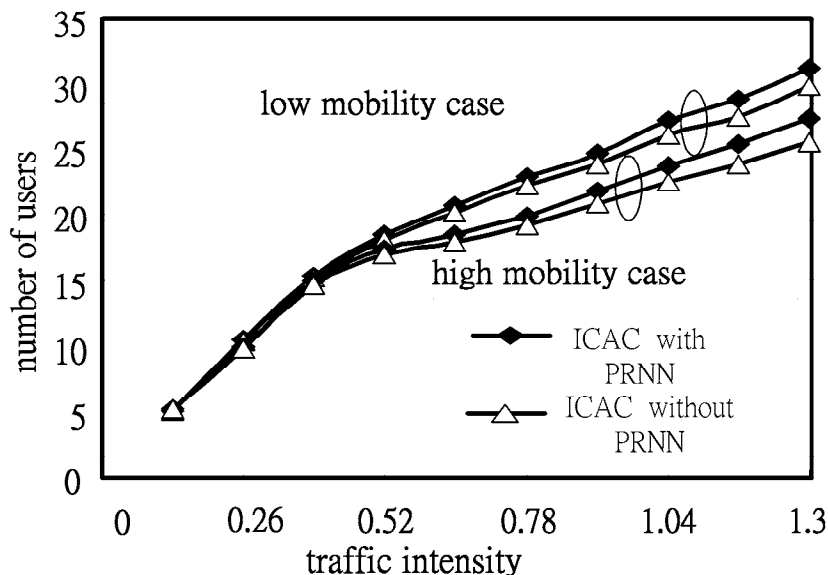


Figure 3.4: The mean number of accommodation users versus traffic intensity for ICAC with and without PRNN interference predictor.

We first demonstrate the effects of the adoption of PRNN interference prediction and

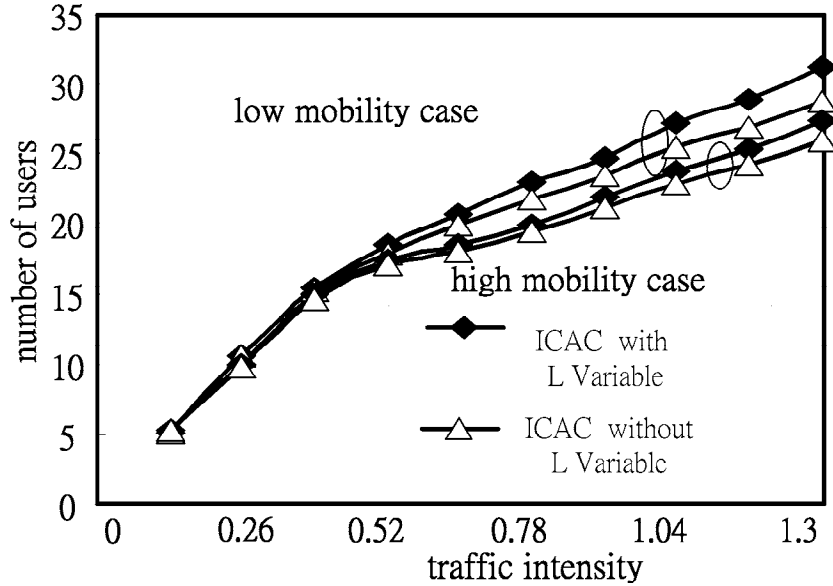


Figure 3.5: The mean number of accommodation users versus traffic intensity of ICAC with and without link gain L variable.

the link gain on the system capacity. Fig. 3.4 shows the mean number of accommodation users versus the traffic intensity ρ for ICAC with and without PRNN interference predictor. It can be found that in the low mobility case, the ICAC equipped with PRNN interference predictor can attain maximal 5% gain of system capacity at $\rho = 1.3$, compared with the ICAC without PRNN interference predictor. In the high mobility case, the gain of system capacity achieved by ICAC with PRNN interference predictor is above 5% after $\rho \geq 0.91$. The gain of system capacity increases along with the increment of traffic load; and the gain of system capacity in high mobility case is more than that in low mobility case. The larger the variance of interference power received at the base station is, the more significantly the PRNN interference predictor can facilitate the estimation.

Fig. 3.5 shows the mean number of accommodation users versus traffic intensity for ICAC with and without link gain L variable. In the low mobility case, the system capacity of ICAC with link gain achieves improvement by above 5% more than that of

ICAC without link gain as $\rho \geq 0.78$. In the high mobility case, the gains of system capacity are 2.5% as $\rho = 0.78$ and about 5% as $\lambda = 1.3$. And the capacity gain increases as the traffic load becomes heavy in both low and high mobility cases. It is because the ICAC scheme with L can reject bad users and accept good users at heavy traffic conditions, while the ICAC scheme without L variable has no such information to make decision. But in the high mobility case, the capacity gain is reduced since good users are more likely to become bad users and the interference will deteriorate. Moreover, the ICAC with the link gain variable can implicitly avoid over interfering adjacent cells. As noted, the predicted interference received at base station reflects partly the traffic load of the adjacent cells; and ICAC rejects the highly interfered users (bad users) to avoid serious interference to the adjacent cells if the predicted interference is large. We have simulated the case of hot spot. The result shows that the hot spot cells are not too aggressive to suppress the the accommodation users in the adjacent cells. Therefore, ICAC with the link gain variable has taken the interference of adjacent cells into considerations.

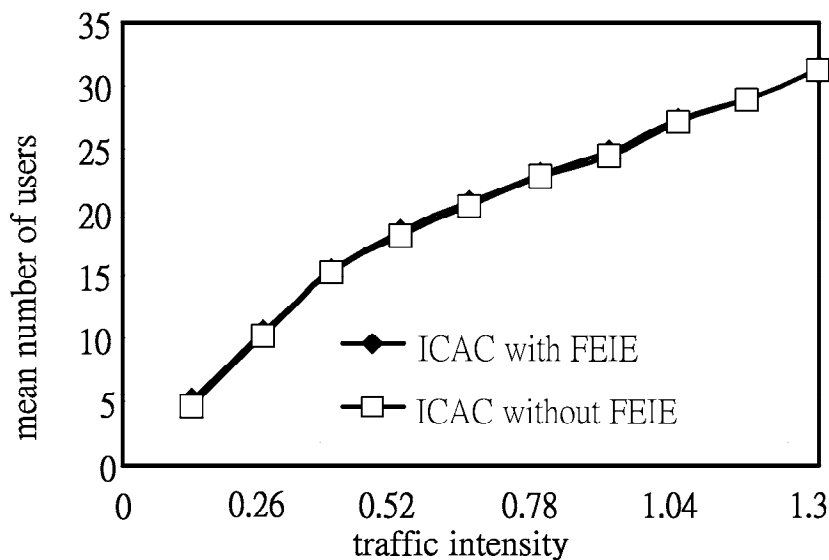


Figure 3.6: The mean number of accommodation users versus traffic intensity of ICAC with and without FEIE.

Fig. 3.6 show the number of accommodation users versus traffic intensity for ICAC with and without fuzzy equivalent interference estimator (FEIE). The ICAC without FEIE is simulated by feeding the equivalent interference obtained in the Appendix to the fuzzy call admission processor. It can be found that they have the similar performance. However, the former uses simple logic to get the equivalent interference, while the later obtains the equivalent interference by complicated computation.

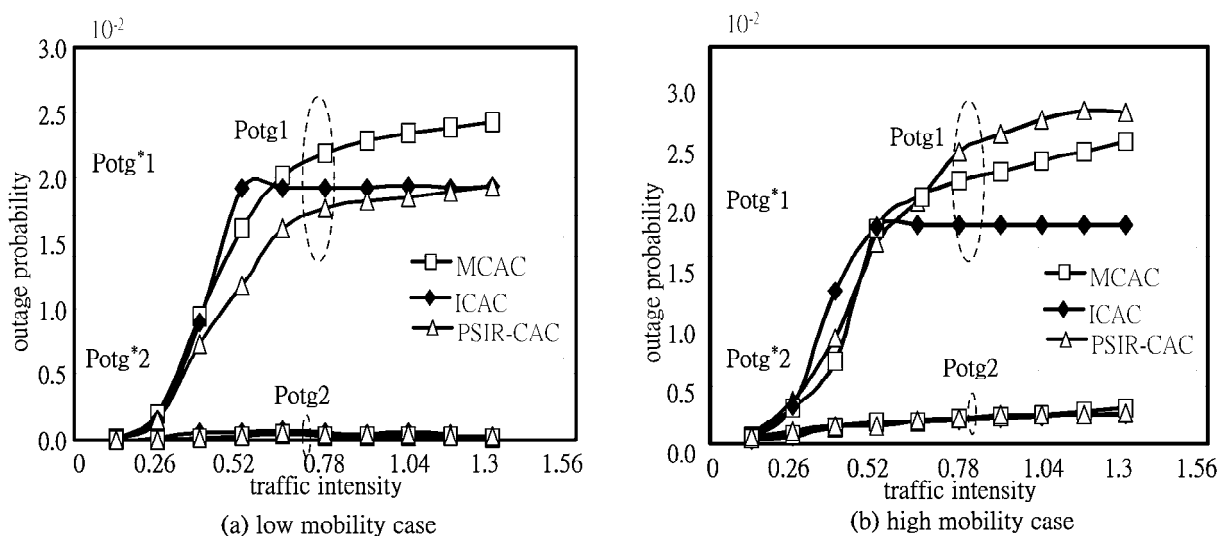


Figure 3.7: Outage probabilities versus traffic intensity.

Fig. 3.7 illustrates the outage probabilities versus traffic intensity for ICAC, MCAC, and PSIR-CAC in (a) low and (b) high mobility cases. It can be seen that ICAC can always guarantee QoS requirements of outage probabilities for all traffic types and all traffic load conditions; PSIR-CAC cannot keep the type-1 outage probability guaranteed in the high mobility case due to the more un-predictable change of interference received at the base station; and MCAC cannot guarantee the type-1 outage probabilities as traffic load gets heavier in both low and high mobility cases. It can also be found that the outage probability of ICAC is the highest in the QoS-guaranteed region ($\rho \leq 0.52$) than those in other two schemes, and is almost kept constant at 0.02 after $\rho > 0.52$. It is

because that ICAC adopts intelligent techniques such as fuzzy logic systems and neural networks, which have powerful reasoning capabilities and learning ability, respectively, to cope with the variant interference of uncertain traffic; and ICAC adopts measures of the outage probabilities of each type of traffic as input linguistic variables. But MCAC and PSIR-CAC do not take the outage probability and system load variation into account. ICAC can adapt to fluctuating traffic load situations and fulfill the requirements.

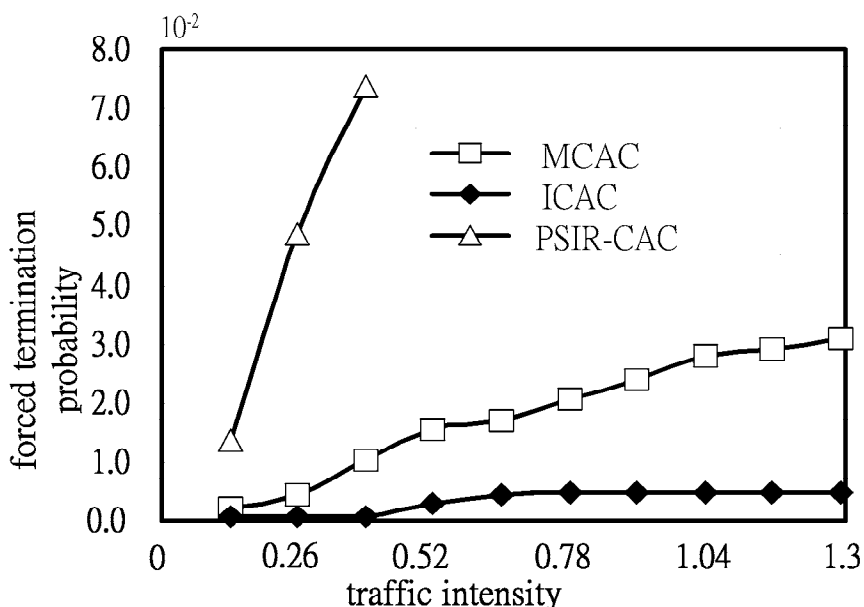


Figure 3.8: The forced termination probabilities versus new call arrival rate.

Fig. 3.8 shows the forced termination probability of handoff call requests versus traffic intensity for ICAC, MCAC, and PSIR-CAC in low mobility case. It can be found that ICAC can always keep the forced termination probability of handoff calls under the constraint no matter how the traffic load is; MCAC, which simply sets the priority for handoff call over new call, cannot always guarantee the forced termination probability requirement except that the admission margin parameter for handoff calls in MCAC is adjusted for different traffic conditions; and PSIR-CAC extremely violates the constraint because it does not take this constraint into considerations.

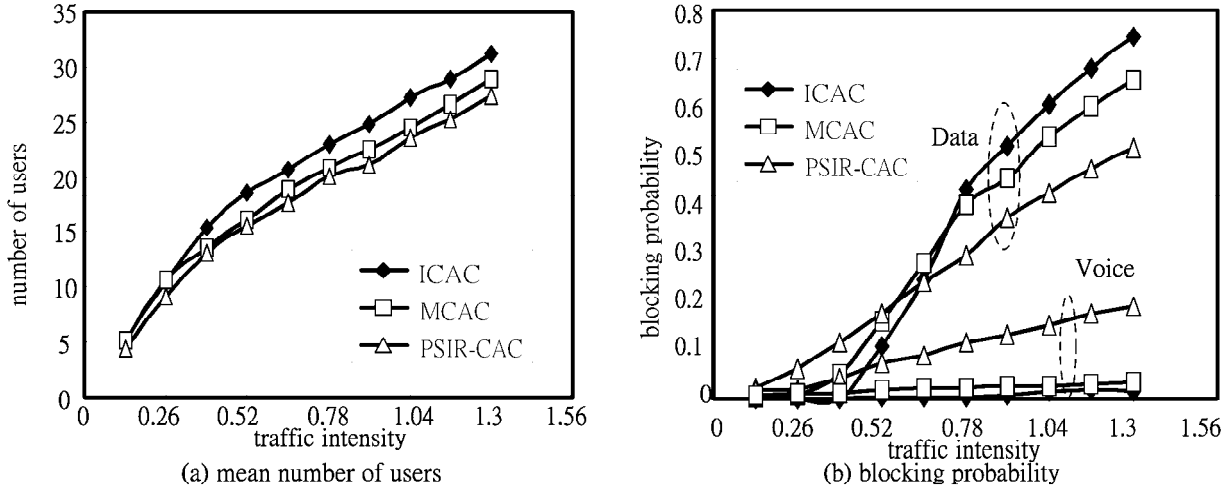


Figure 3.9: The number of accommodation users (a) and the new call blocking probability (b) versus traffic intensity in low mobility case.

Fig. 3.9 illustrate (a) the number of users and (b) the new call blocking probabilities of voice and data users versus traffic intensity for ICAC, MCAC, and PSIR-CAC in low mobility case. It can be found that ICAC accepts users more than PSIR-CAC and MCAC by an amount of around 13% and 10%, respectively. And in the $\rho \leq 0.52$ region where all these three schemes can keep QoS guaranteed, the blocking probability of ICAC is the lowest; but out of the region, say $\rho \geq 0.78$, the blocking probability of data users for ICAC is the largest, while that of voice users for ICAC is still the smallest. This is because, as $\rho \leq 0.52$, ICAC can precisely predict the system load condition and thus fully utilize the resource; but in the heavy-load condition, ICAC tends to reject bad users, hence the adjacent cell interference is significantly reduced and the system capacity grows up continuously. Notice that the equivalent interference of data connection is larger due to the higher burstiness and the stricter requirement, and they are likely to be bad users. In the high mobility case, similar phenomena are observed.

Fig. 3.10 shows (a) the number of accommodation data users and (b) the blocking

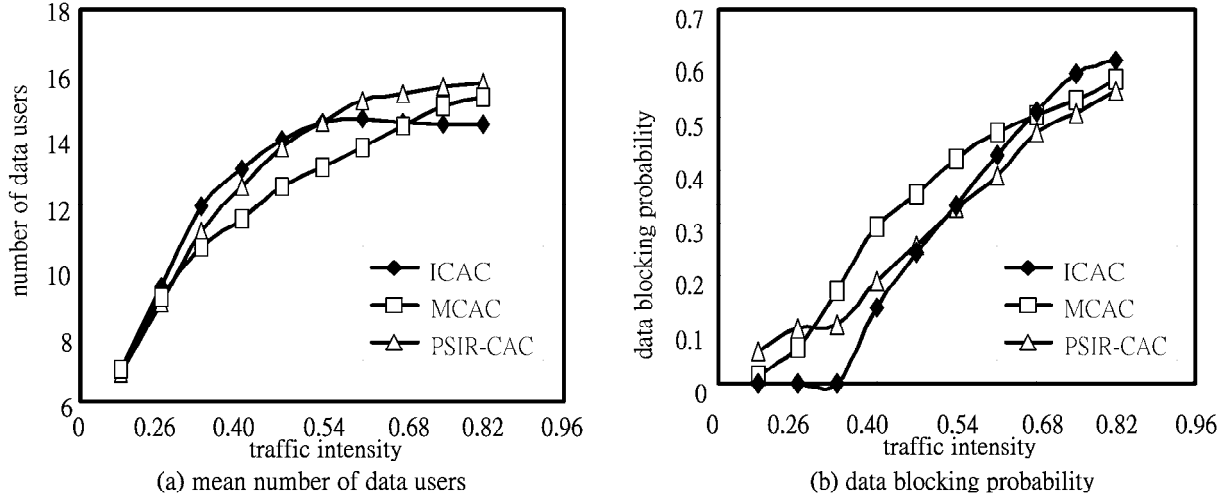


Figure 3.10: the number of accommodation data users (a) and the blocking probability of data users (b) versus the new call arrival rate of data users where voice arrival rate is fixed at 0.1 per frame time.

probability of data users versus traffic intensity of data users where the voice arrival rate is fixed to be 0.1 per frame time and no voice users are allowed to be blocked. It can be seen that the mean number of accommodation data users of ICAC is 7% and 11% more than those of MCAC and PSIR-CAC at $\rho < 0.40$ where all these three schemes can guarantee the requirements of outage probabilities. As $0.40 \leq \rho \leq 0.54$ where MCAC and PSIR-CAC begin to violate the QoS requirements, ICAC still attains more number of data users by the amount 5% and 9% than MCAC and PSIR-CAC, respectively. After $\rho \geq 0.54$, the accommodation data users of ICAC remains constant in order to keep QoS requirements guaranteed and the blocking probability of ICAC grows higher than those of MCAC and PSIR-CAC, while the numbers of data users of MCAC and PSIR-CAC continue increasing but their QoS requirements keep deteriorating. Therefore, it can be concluded that ICAC can precisely estimate the system condition to admit more users than MCAC and PSIR-CAC as these three schemes satisfy the QoS requirements; and ICAC accepts reasonable users into the system to keep the requirement guaranteed while

the MCAC and PSIR-CAC violate the requirement.

3.6 Concluding Remarks

This chapter presents an intelligent call admission controller (ICAC) for wideband CDMA cellular systems to support differentiated QoS provisioning, satisfy the system QoS constraints, and maximize the spectrum utilization. ICAC is applied with both fuzzy logic control and pipelined recurrent neural network (PRNN) techniques, thus contains a fuzzy equivalent interference estimator, a PRNN interference predictor, and a fuzzy call admission processor. The fuzzy equivalent interference estimator determines the interference power caused by the new call request, based on the domain knowledge on effective bandwidth method. The PRNN interference predictor forecasts the system interference mean at the next time period, and it can achieve additional gain in system capacity by an amount of 5%. The fuzzy call admission processor considers the system QoS performance measures of each traffic type and the link gain of the call request to determine whether to accept the call request, based on the estimated equivalent interference generated by the call and the predicted next-step interference caused by existing calls. The further consideration of the variable of link gain of the new call request can make ICAC capable of rejecting bad users and accepting good users to improve the system capacity. Therefore, ICAC can achieve system capacity higher than PSIR-CAC and MCAC by an amount of more than 10% in regions where QoS requirements are guaranteed. ICAC is indeed effective for differentiated QoS provisioning for wireless multimedia CDMA systems.